CrossMark

RHINOLOGY

Numerical simulation of humidification and heating during inspiration in nose models with three different located septal perforations

Jörg Lindemann[1] · Michael Reichert[1] · Ralf Kröger[2] · Patrick Schuler[1] · Thomas Hoffmann[1] · Fabian Sommer[1]

Abstract Nasal septum perforations (SP) are characterized by nasal obstruction, bleeding and crusting. The disturbed heating and humidification of the inhaled air are important factors, which cause these symptoms due to a disturbed airflow. Numerical simulations offer a great potential to avoid these limitations and to provide valid data. The aim of the study was to simulate the humidification and heating of the inhaled air in digital nose models with three different SPs and without SP. Four realistic bilateral nose models based on a multi-slice CT scan were created. The SP were located anterior caudal, anterior cranial and posterior caudal. One model was without SP. A numerical simulation was performed. Boundary conditions were based on previous in vivo measurements. Heating and humidification of the inhaled air were displayed, analyzed in each model and compared to each other. Anterior caudal SPs cause a disturbed decrease of temperature and humidity of the inhaled air. The reduced temperature and humidity values can still be shown in the posterior nose. The anterior cranial and the posterior caudal perforation have only a minor influence on heating and humidification. A reduced humidification and heating of the air can be shown by numerical simulations due to SP depending on their localization. The anterior caudal SP representing a typical localization after previous surgery has the biggest influence on heating and humidification. The results explain the typical symptoms such as crusting by drying-out the nasal mucosa. The size and the localization of the SP are essential for the symptoms.

Keywords Septal perforation · Humidification · Temperature · Numerical simulation · Computational fluid dynamics

J. Lindemann and M. Reichert contributed equally and shared authorship.

✉ Michael Reichert
  michael.reichert@uniklinik-ulm.de

1   Department of ORL, Head and Neck Surgery,
    Ulm University Medical Center, Frauensteige 12,
    89075 Ulm, Germany

2   ANSYS Germany GmbH, Darmstadt, Germany

Introduction

Nasal septum perforation (SP) is a not-infrequently seen clinical picture in an ENT department. The most common reason for a SP is still previous septal surgery [1–5]. Other reasons are cauterization, packing, septal abscess or hematoma, Wegener's granulomatosis and nasal drug abuse.

SPs are characterized by subjective nasal obstruction, dryness, crusting, epistaxis and whistling. These symptoms are mainly caused by disturbed airflow and intranasal air conditioning. In previous studies, nasal airflow, temperature and humidity were measured either in physical nose models (so called Mink's boxes) [6] or in vivo [7, 8]. Both methods have their disadvantages. While Mink's boxes are only able to show airflow patterns, in vivo measurements are limited by the narrow anatomical structures of the nose and by the confined temporal and spatial resolution.

Nowadays numerical simulations are well established and standardized [9–16]. Computational fluid dynamics (CFD) are able to visualize the relationship between intranasal airflow pattern characteristics in combination with air temperature and humidity under various

conditions. Studies based on CFD simulations were able to show airflow patterns, temperature and humidity distribution in nose models of healthy noses [9, 14–17]. In nose models with SP, several pathologies could be shown. Disturbed airflow patterns mainly in the area of the posterior margin of the SP are responsible for the crusting in this region. Huge vortices cause the subjective nasal obstruction in patients with SP [10–13]. SPs are frequently located in the anterior caudal cartilaginous part of the septum after previous surgery and cause more symptoms than the SPs, which are located more cranial or more posterior. In a former study, we could show that airflow patterns are particularly influenced by anterior caudal localized perforations. Perforations in the cranial and posterior parts of the septum play a subordinate role [13].

Therefore, the objective of this study was to show the influence of the exact site of the SP on nasal air conditioning. A numerical simulation was performed to investigate humidification and heating as a function of airflow during a dynamic respiratory cycle.

Materials and methods

Nose models

To build a three-dimensional (3D) computational bilateral nose model a CT scan of a healthy 50-year-old male was used. The patient had no pathology concerning the nasal septum, paranasal sinuses and no history of nasal disease or allergy.

The CT scan was performed by a Philips Brilliance 16 (Philips International BV, Amsterdam, the Netherlands). The slices had a thickness of 1.3 mm, increment 6 mm. The total number of slices was 241. The coronary plane was reconstructed using a slice thickness of 1 mm. We used ScanIP version 4.0 and ScanFE version 3.2.3 (Simpleware Ltd., Exeter, United Kingdom) for the segmentation. Frontal sinuses were excluded as they do not have any effect on nasal airflow patterns. The ethmoid sinus was included to simulate a realistic middle meatus.

After creating this standard model without a SP we used the same model as a basis to create three more models with different located SPs (anterior caudal, anterior cranial and posterior caudal) (Fig. 1). These modifications and additional changes regarding the mesh quality were performed using ANSYS T-Grid (ANSYS Inc.). Each of the created models consisted of about 9 million cells and between 2.4 and 2.6 million polyhedral after the meshing process. The minimum orthogonal quality was $1.05563e^{-01}$ and the maximum aspect ratio was 2.84465.

Numerical simulation

The numerical simulations were performed by ANSYS Fluent (14.0.0, ANSYS Workbench 14, ANSYS, Inc.). The boundary conditions were based on the experiences our study group obtained previously by in vivo measurements and numerical simulations [7, 8, 10, 13, 14, 17–23].

The breathing had a frequency of 14.3 gasps per minute with inspiration taking 1.9 s and expiration 2.3 s (4.2 s for one complete cycle). In contrast to previous studies, a

Fig. 1 Nose models with three different located SPs. **a** nose model without SP, **b** anterior caudal SP, **c** anterior cranial SP, **d** posterior caudal SP (*SP* septal perforation)
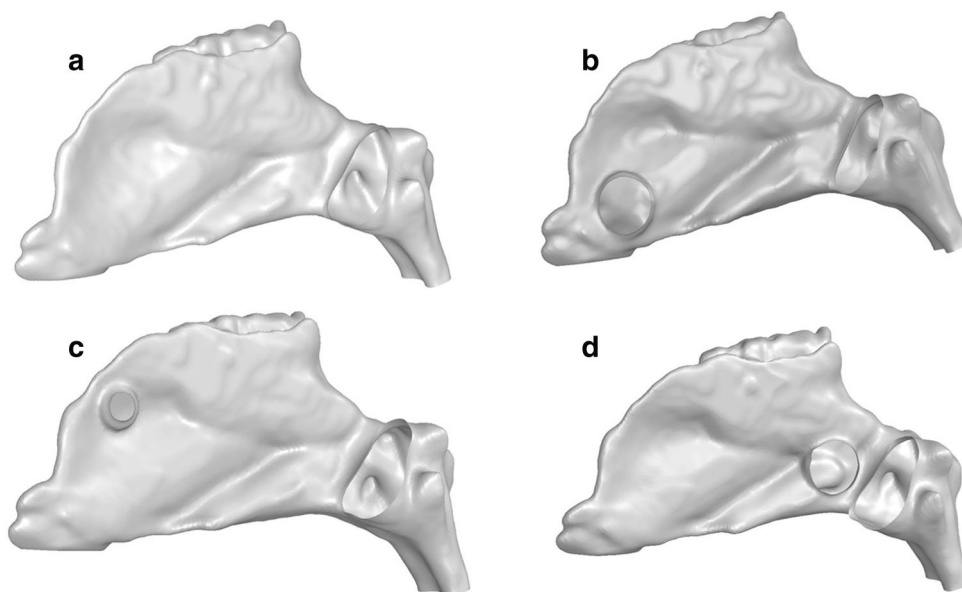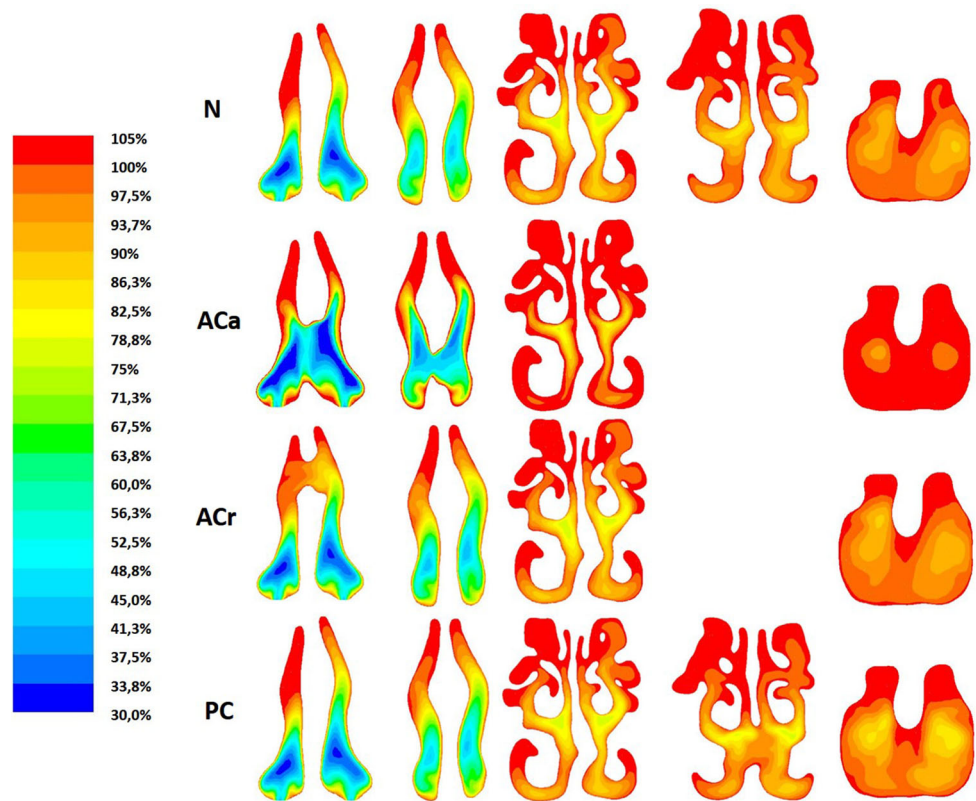
Fig. 2 Relative humidity in percent during maximal inspiratory airflow. *N* model without SP, *ACa* anterior caudal perforation, *ACr* anterior cranial perforation, *PC* posterior caudal perforation

dynamic breathing cycle was simulated. The inspired air had a temperature of 20 °C (293 K) and 30 % relative humidity. The temperature of the nasal mucosa decreased during the inspiration from 34 °C (307 K) to 30 °C (303 K) at the end of the cycle. The moisture of the nasal mucosa was set to be constant at 100 % because of the assumption of the presence of a steady mucus film. The expired air had a temperature of 35 °C (308 K) and a relative humidity of 100 %. The temperature of the nasal mucosa increased from 30 °C (303 K) to 34 °C (307 K). To simulate the inspiration a negative pressure as set in the nasopharynx between 0 and −10 Pa. This led to a flow speed of up to 2 m/s around the middle turbinate. For the expiration, the pressure in the nasopharynx was set between 0 and 10 Pa.

Target parameters of the numerical simulation were intranasal air humidity (relative humidity in %) and temperature [in Kelvin (K)] values. All results are illustrated in coronary cutting planes.
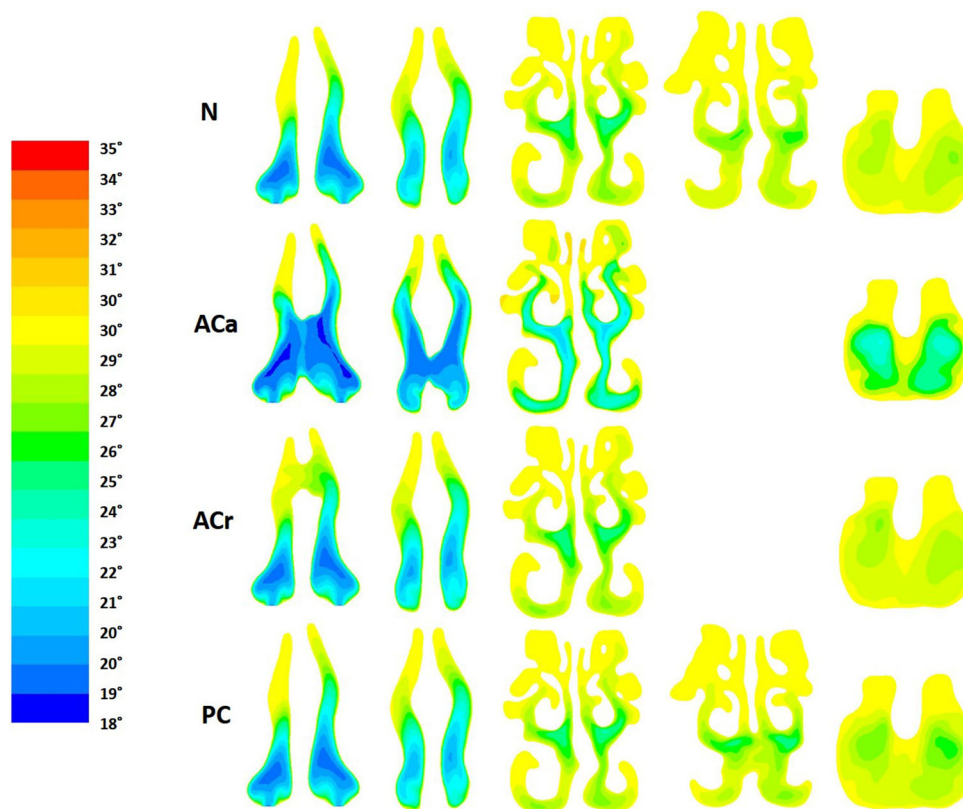
Results

The results for relative humidity in all four nose models are shown in Fig. 2. In the upper row the results for the nose model without SP are shown in five coronary cutting planes. The first three planes visualize the anterior part of the nose, the fourth plane is located in the middle of the nose and the fifth plane visualizes the nasopharynx. It is clearly shown that relative humidity is lowest in the anterior caudal part of the nose. Humidity does not change much during inspiration in the cranial parts of the nose. Relative humidity reaches high levels of saturation in the middle and posterior parts of the nose.

The results for the anterior caudal perforation are also shown in Fig. 2, second row. While in the first layer, which represents the center of the perforation, only slight differences in humidification can be shown; there are clear differences at the posterior margin of the SP (layer 2). The area in which humidity reaches only values around 40–45 % relative saturation is much bigger than in the healthy nose. In the middle part of the nose, directly behind the perforations relative humidity is even higher than in the healthy nose model (layer 3). This effect can also be seen in the nasopharynx (layer 5).

As mentioned above, humidity does not change much in the cranial parts of the nose. Therefore only slight differences in humidification can be shown in the nose model with the anterior cranial perforation (third row). Due to high saturation in the posterior parts of the nose during inspiration the posterior caudal SP also does not relevantly influence the humidification during inspiration (fourth row).

Fig. 3 Temperature in °C
during maximum inspiratory
airflow. *N* model without SP,
ACa anterior caudal perforation,
ACr anterior cranial perforation,
PC posterior caudal perforation

The results for temperature in all four nose models
are shown in Fig. 3. The upper row again shows the
temperature in the nose model without SP. The lowest
temperature during maximum inspiration is in the
anterior caudal parts of the nose. Due to lack of flow,
the temperature in the cranial parts of the nose is not
decreased by inspiration. Temperature increases during
passing the middle turbinate and reaching the middle
and posterior parts of the nose. The second row of
cutting planes in Fig. 3 shows the results for the nose
model with the anterior caudal perforation. Decreased
temperature can already be shown in the first layer.
There are also clear differences in temperature in the
second and third layers, which represent the posterior
margin of the anterior caudal perforation and the area
directly behind the perforation. Those differences can
still be seen in the middle and posterior parts of the nose
(layer 5). As mentioned above, temperature does not
decrease much in the cranial parts of the anterior nose.
Therefore, no clear differences of heating the inhaled air
can be shown in the model with the anterior cranial
perforation (third row). Likewise, no clear differences
can be shown in the model with the posterior caudal
perforation (fourth row).

Discussion

Due to the fast increase of computational processing power
numerical simulations become more and more important to
understand pathologies within the nose. About 10 years
ago physiological knowledge about intranasal airflow pat-
terns, temperature and humidity was obtained either by
in vivo measurements with thermocouples [7, 8, 22–26] or
by measurements in physical nose models, so called
Mink's boxes [6, 27]. However, these measurements had
several disadvantages due to limited space within the
human nose. Furthermore, in vivo measurements could
only be performed on several defined points within the
nose. The spatial resolution was poor. The disadvantage of
the Mink's boxes was that they did not provide any insights
into the temperature and humidification of the inspired air.

Nowadays many studies about numerical simulations
are published. The early studies used unilateral nose
models due to reduced computational processing power
[28, 29]. The simulations were performed assuming a
constant inflow of the air [9–13, 29].

Numerical simulations became well established and
standardized during the past years. Our study group has
gained a lot of experience by numerous performed

simulations [9, 10, 13, 14, 17–20]. The set boundary conditions correlate well with in vivo measurements and can be considered as valid.

In this study, we performed numerical simulations on four different bilateral realistic nose models, one without pathology and three with different located septal perforations. Realistic breathing cycles were simulated, which means variable values for the air velocity of the inhaled air as well as variable values for the temperature of the nasal mucosa to provide physiological conditions. Furthermore, we investigated the intranasal air temperature and humidity, which is an approach that did not exist previously. Former studies have mainly investigated the airflow patterns and the shear stress values in the area of the SP [11–13]. Only one study of our working group investigated the air temperature distribution within a nose model presenting a septal perforation, the humidity was not considered [10].

Grant et al. [12] showed that the skin friction was larger in the model with the septal perforation especially concentrated around the perforation area. Furthermore, the relatively high velocity flow was observed along the perforation and high shear stress values occurred at the posterior end of the perforation. Lee et al. [11] performed numerical simulations on nose models with different sized septal perforations. Grant et al. observed high shear stress values in the posterior region of the SP. Furthermore Lee et al. observed a flow exchange through the SP, from the higher flow rate to the lower flow rate nostril side. This effect was shown mainly in the large and medium size SP. Our study group [13] investigated the influence of the location of SP on airflow patterns. We could show that mainly anterior caudal SP influence the airflow patterns by causing turbulent kinetic energy within the SP. Cranial and posterior located SPs have a smaller influence on the airflow.

As mentioned above, knowledge about the temperature and humidity profile within SP is rare. We [7, 8] performed two in vivo studies to investigate these parameters comparing healthy volunteers and patients with SP as well as before and after surgical closure of SP. We observed a significantly reduced increase of humidity in patients with SP compared to the healthy volunteers. The patients with SP suffered significantly more from nasal dryness. Postoperatively the increase of temperature and humidity was significantly higher than preoperatively.

So far, there is only one numerical simulation regarding the temperature profile in patients with SP [10]. In this study high-velocity values were observed in the area of the SP analog to the other studies mentioned above. In those areas of high velocity the air temperature was decreased due to a reduced contact to the nasal mucosa. This finding shows the close connection between airflow, air velocity and temperature.

In our study we investigated the temperature and the humidity in three different SPs. According to the findings of Pless et al. we could also show a relevant decreased temperature profile in the anterior caudal perforation. Furthermore, relative humidity also decreased in the anterior part of the nose in the model with anterior caudal SP. In the middle and posterior parts of the nose relative humidity even slightly increased compared to the healthy nose model. We see the reason for the detected increase of relative humidity in the close relation between temperature and humidity. Relative humidity is the amount of water vapor in the air depending on its temperature. It represents a function of temperature. Absolute humidity is the water content of air. Therefore, the simulated decreased air temperature leads to a decreased "absolute" humidity in the nose model with the anterior caudal perforation due to a reduced water content. The other two septal perforations (anterior cranial and posterior caudal) did not have such a significant influence on humidity and temperature.

Conclusion

Our current study confirms the knowledge we achieved from our former studies. Mainly anterior caudal SPs come along with decreased air temperature and decreased humidity in the anterior parts of the nose, which leads to dehydration, crusting and epistaxis, the main symptoms of SPs. The posterior parts of the nose seem not to be substantially affected. Perforations which are located cranial or posterior have only a minor influence on temperature and humidity. Therefore, it seems reasonable to perform surgery on anterior caudal septal perforations, even if the perforation might only relocated to a more cranial or more posterior part of the nose and a complete closure might not be achieved due to the size of the perforation.

References

1. Schultz-Coulon HJ (1997) Septumverschlussplastiken nach der Brückenlappentechnik bei 126 Patienten–eine Analyse. Laryngorhinootologie 76(8):466–474
2. Fairbanks DN, Fairbanks GR (1980) Nasal septal perforation: prevention and management. Ann Plast Surg 5(6):452–459
3. Teymoortash A, Hoch S, Eivazi B et al (2011) Experiences with a new surgical technique for closure of large perforations of the nasal septum in 55 patients. Am J Rhinol Allergy 25(3):193–197
4. Pedroza F, Patrocinio LG, Arevalo O (2007) A review of 25-year experience of nasal septal perforation repair. Arch Facial Plast Surg 9(1):12–18
5. Becker SS, Dobratz EJ, Stowell N et al (2008) Revision septoplasty: review of sources of persistent nasal obstruction. Am J Rhinol 22(4):440–444

6. Mlynski G, Grützenmacher S, Plontke S et al (2001) Correlation of nasal morphology and respiratory function. Rhinology 39(4):197–201

7. Lindemann J, Kühnemann S, Stehmer V et al (2001) Temperature and humidity profile of the anterior nasal airways of patients with nasal septal perforation. Rhinology 39(4):202–206

8. Lindemann J, Leiacker R, Stehmer V et al (2001) Intranasal temperature and humidity profile in patients with nasal septal perforation before and after surgical closure. Clin Otolaryngol Allied Sci 26(5):433–437

9. Pless D, Keck T, Wiesmiller K et al (2004) Numerical simulation of air temperature and airflow patterns in the human nose during expiration. Clin Otolaryngol Allied Sci 29(6):642–647

10. Pless D, Keck T, Wiesmiller KM et al (2004) Numerical simulation of airflow patterns and air temperature distribution during inspiration in a nose model with septal perforation. Am J Rhinol 18(6):357–362

11. Lee HP, Garlapati RR, Chong VFH et al (2010) Effects of septal perforation on nasal airflow: computer simulation study. J Laryngol Otol 124(1):48–54

12. Grant O, Bailie N, Watterson J et al (2004) Numerical model of a nasal septal perforation. Stud Health Technol Inform 107(Pt 2):1352–1356

13. Lindemann J, Rettinger G, Kröger R et al (2013) Numerical simulation of airflow patterns in nose models with differently localized septal perforations. Laryngoscope 123(9):2085–2089

14. Sommer F, Kroger R, Lindemann J (2012) Numerical simulation of humidification and heating during inspiration within an adult nose. Rhinology 50(2):157–164

15. Garcia GJM, Bailie N, Martins DA et al (2007) Atrophic rhinitis: a CFD study of air conditioning in the nasal cavity. J Appl Physiol 103(3):1082–1092

16. Naftali S, Rosenfeld M, Wolf M et al (2005) The air-conditioning capacity of the human nose. Ann Biomed Eng 33(4):545–553

17. Lindemann J, Keck T, Wiesmiller K et al (2006) Nasal air temperature and airflow during respiration in numerical simulation based on multislice computed tomography scan. Am J Rhinol 20(2):219–223

18. Lindemann J, Keck T, Wiesmiller KM et al (2005) Numerical simulation of intranasal air flow and temperature after resection of the turbinates. Rhinology 43(1):24–28

19. Lindemann J, Brambs H, Keck T et al (2005) Numerical simulation of intranasal airflow after radical sinus surgery. Am J Otolaryngol 26(3):175–180

20. Lindemann J, Keck T, Wiesmiller K et al (2004) A numerical simulation of intranasal air temperature during inspiration. Laryngoscope 114(6):1037–1041

21. Wiesmiller K, Keck T, Leiacker R et al (2007) Simultaneous in vivo measurements of intranasal air and mucosal temperature. Eur Arch Otorhinolaryngol 264(6):615–619

22. Lindemann J, Keck T, Scheithauer MO et al (2007) Nasal mucosal temperature in relation to nasal airflow as measured by rhinomanometry. Am J Rhinol 21(1):46–49

23. Lindemann J, Leiacker R, Rettinger G et al (2002) Nasal mucosal temperature during respiration. Clin Otolaryngol Allied Sci 27(3):135–139

24. Keck T, Leiacker R, Heinrich A et al (2000) Humidity and temperature profile in the nasal cavity. Rhinology 38(4):167–171

25. Keck T, Leiacker R, Riechelmann H et al (2000) Temperature profile in the nasal cavity. Laryngoscope 110(4):651–654

26. Keck T, Leiacker R, Lindemann J et al (2001) Endonasales Temperatur- und Feuchteprofil nach Exposition zu verschieden klimatisierter Einatemluft. HNO 49(5):372–377

27. Grützenmacher S, Mlynski R, Lang C et al (2005) The nasal airflow in noses with septal perforation: a model study. ORL J Otorhinolaryngol Relat Spec 67(3):142–147

28. Hörschler I, Brücker C, Schröder W et al (2006) Investigation of the impact of the geometry on the nose flow. Eur J Mech B Fluids 25(4):471–490

29. Keyhani K, Scherer PW, Mozell MM (1995) Numerical simulation of airflow in the human nasal cavity. J Biomech Eng 117(4):429–441